

Zonally Propagating Modes of the Global East-West Circulation Associated with the Southern Oscillation

By Tetsuzo Yasunari*

Department of Meteorology, Florida State University, Tallahassee, FL 32306

(Manuscript received 13 June 1985, in revised form 14 October 1985)

Abstract

The global-scale east-west circulation in the tropics associated with the Southern Oscillation (SO) was investigated by using two different data sets (FSU data and NMC data), which contain about 20 years of tropical wind field observations.

As a predominant mode of the interannual time scale, the eastward-propagating anomalous divergent circulation (with a phase speed of 6° - 10° longitude month⁻¹) was found to be on the time scale of the SO (40-60 month period) with a zonal wavenumber-one structure. The eastward propagation is most prominent over the Indian Ocean toward the eastern Pacific. This mode shows a large amplification over the Indonesian maritime continent through the eastern Pacific, which may correspond with the modulation of the local Walker circulation.

Another east-west oscillation with a similar zonal structure but a faster eastward propagation (12° - 15° longitude month⁻¹) was also noted with the quasi-biennial (QBO) time scale (20-30 month period). In addition, these two modes show a coupling (decoupling) of the anomalies which seems to be associated with the occurrence of the major (minor) El Niño events over the central through the eastern equatorial Pacific.

1. Introduction

The Southern Oscillation (SO) is well known as a standing oscillation of the surface pressure between the Indian Ocean through Indonesia and the eastern south Pacific with a period of several years. A minimum phase of this pressure oscillation is coupled with high sea surface temperature (SST) anomalies over the central through eastern equatorial Pacific called "El Niño" events. These atmosphere-ocean coupled circulation anomalies are currently called the El Niño/Southern Oscillation (ENSO) events. In recent years, these phenomena have been noted by many authors (Horel and Wallace, 1981 *etc.*) as important modulators of the climatic anomalies of the northern high latitudes through the Rossby

wave response to the high SST anomalies over the equatorial Pacific.

In the tropical troposphere, this oscillation manifests itself as a zonally-oriented direct (heat-induced) circulation cell along the equatorial Pacific, *i.e.* the "Walker circulation" (Bjerknes, 1969). In a mean state, the upward motion is located over the warm, moist Indonesian maritime continent, whereas the downward motion is located over the relatively cool and dry central through eastern Pacific. The circulation cell along the equatorial plane is extremely weak at the minimum phase (*i.e.*, El Niño phase) of the SO.

It has been noted that this local Walker circulation is characterized as a part of the global east-west circulation as shown by Krishnamurti (1971) and Krishnamurti *et al.* (1973). In spite of the numerous observational and theoretical studies on the typical phases

* Present affiliation: Institute of Geoscience, University of Tsukuba, Ibaraki 305, Japan.

of the ENSO events and their influences on higher latitudes, few studies have examined how the east-west circulations in the tropics modulate or are modulated by the ENSO events. We believe that this aspect of the SO is very important to understand the mechanism of the SO, since the change in the planetary-scale east-west circulation greatly affects the total energy generation and conversion in the tropical motion field (Krishnamurti *et al.*, 1973; Kanamitsu and Krishnamurti, 1978). The present study focuses on this problem and will show some preliminary observational results on the zonal structure of the global east-west circulation associated with the SO.

2. Data

The first data set to be used in this study is derived from the U.S. National Meteorological Center's (NMC) operational tropical wind field analysis. This analysis consists of zonal and meridional wind components of the wind at six levels on a Mercator grid with a longitude spacing of 5° . The latitudinal boundaries are 48.1°N and 48.1°S and the full grid contains 1656 (23×72) points. The monthly mean data is available for the period March 1968 to February 1985.

Although three different interpolation techniques were used during the period, Arkin (1982) noted the minor effects on the large-scale features of the mean monthly fields. However, it should be noted that the Hough analysis, which is essentially non-divergent, was applied during the period September 1974 to August 1978.

We utilized the wind field at 200 mb as representative of the upper troposphere. The data for 850 mb and 1000 mb does not adequately cover the analysis period (with less than ten years), but a correlation between the winds at 850 mb and 700 mb during the overlapped period (January 1968 through December 1974) has proven to be very high. The wind field at 700 mb was, therefore, utilized as representative of the lower troposphere.

The second data set to be used is the monthly mean 200 mb wind field of the tropics (45°N - 25°S) analyzed at Florida State University (Pan, 1979). The final analysis of the

monthly data of zonal and meridional wind component is resolved on a $2.5^\circ \times 2.5^\circ$ latitude/longitude grid mesh. The data set was produced by using the least square method to fit more than 180 radiosonde station data to truncated spherical harmonics for wavenumber 0 to 5. The data set covers ten years from January 1965 to December 1974.

Pan (1979) showed a large efficiency of the data set for examining variations of the planetary-scale motions with the interannual time scale. The monthly mean motion field for each month of the whole period is shown in atlas form (Krishnamurti *et al.*, 1983).

The two data sets described above enable us to examine the interannual fluctuations of 200 mb wind field over the global tropics for more than twenty years (January 1965 to February 1985). In addition, the overlapped portion in the time series of data (March 1968 to December 1974) enables us to assess the uniformity and the continuity between these two data sets.

3. Time scale of the Southern Oscillation

Since our main interest is to deduce the zonal structure of the anomalous east-west circulation field associated with the SO, dominant time scales are examined first by the use of the Southern Oscillation Index (SOI). Here the SOI is computed by taking the sea-level pressure difference between Tahiti and Darwin, which is now commonly used as a measure of the intensity of the SO.

Fig. 1 shows the time series of the SOI and Fig. 2 shows the power spectra of the SOI by using the maximum entropy method (MEM). We should note that the dominant periodicity of the SO changes considerably from period to period. For example, during the period of the FSU data set (January 1965 to December 1974), which is hereafter referred to as Period I, a periodicity of about 40 months is a single dominant mode of the SO. During the period of the NMC data set (March 1968 to February 1983), which is hereafter referred to as Period II, the large power exists in a broad periodicity band of 25 to 70 months, but we may distinguish one spectral peak at around 60 months from another peak at

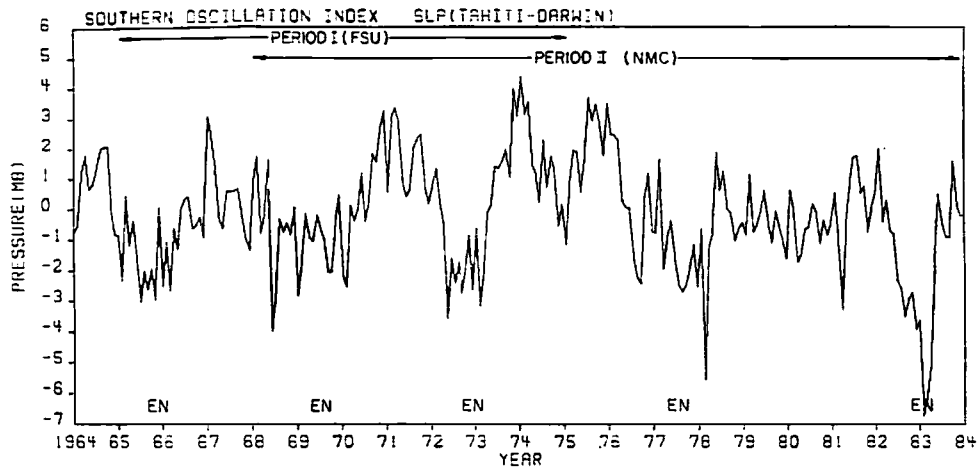


Fig. 1 Southern Oscillation Index from January 1965 to December 1984 defined with the sea-level pressure difference between Tahiti and Darwin. Mean seasonal cycle is subtracted. El Niño event over the eastern Pacific is indicated with "EN". Period of the two data sets are also shown.

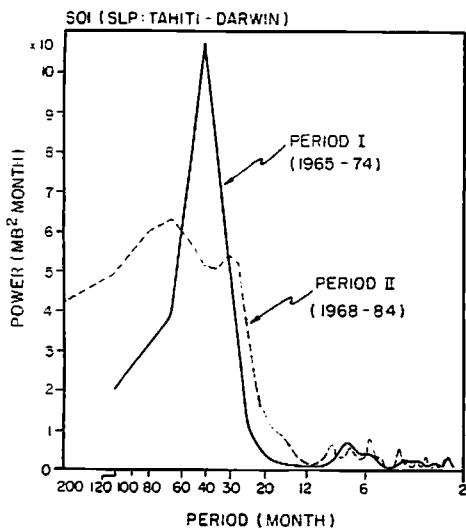


Fig. 2 Power spectra of the Southern Oscillation Index for Period I (FSU data) and Period II (NMC data).

around 30 months. If we refer to the number of occurrence of the minimum SOI phase with El Niño events (see Fig. 1), the former time scale may correspond purely to the SO coupled to El Niño events (or ENSO), while the latter time scale may be related to the quasi-biennial oscillation (QBO) in the tropical troposphere.

It may be an important but difficult problem to determine whether the SO and the QBO in the troposphere are dynamically similar phenomena. Some studies (*e. g.*, Trenberth, 1975; 1976 *etc.*) suggested a different spatial structure of the QBO to that of the SO, while

other studies (*e. g.*, Hastenrath and Wu, 1982 *etc.*) treated this mode as a part of the SO in a broad sense. Some simple dynamical models of the QBO in the troposphere (Brier, 1978; Nicholls, 1978) suggest that the atmosphere-ocean feedback system is somewhat different from that of the SO. For the time being, we will treat these two modes as independent of each other, in reference to the fact that the former is directly coupled to El Niño events in the equatorial Pacific Ocean but the latter is not. The association between these two modes will be discussed further in section 8.

4. Time-space power spectra of the zonal wind

Since the east-west circulation along the tropics may essentially be described with the combination of zonal wind anomalies in the upper and lower troposphere, some time-space characteristics of the zonal wind at 200 mb and 700 mb are examined in the wavenumber-frequency domain.

The time-space power spectral analysis generated using MEM (Hayashi, 1977) was applied to the zonal wind component for Period I and Period II. Before computing the spectra, climatological mean zonal winds for each month were subtracted.

Fig. 3 shows wavenumber-frequency distribution of power spectra at 200 mb. The

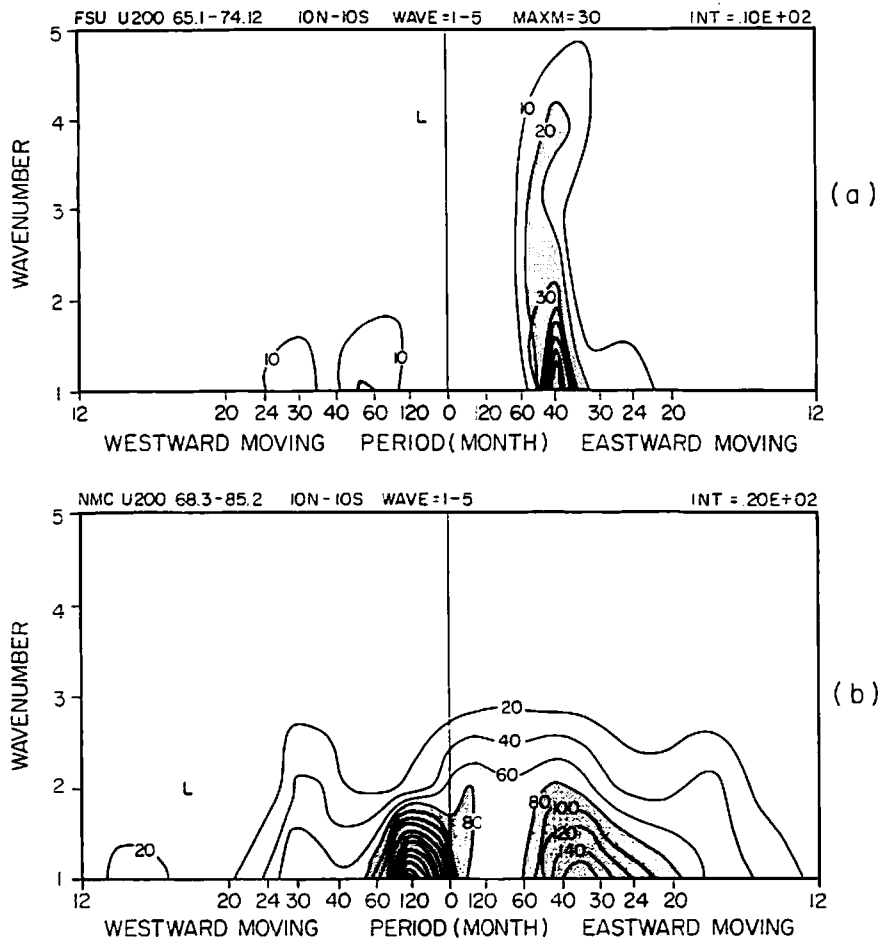


Fig. 3 Wavenumber-frequency distribution of space-time power spectra of zonal wind at 200 mb for (a) Period I (FSU data) and (b) Period II (NMC data). Units are (a) $10 \text{ m}^2 \text{ month}$ and (b) $20 \text{ m}^2 \text{ month}$.

outstanding feature in Period I (Fig. 3(a)) is a concentration of the power to the eastward component of wavenumber one with a period of about 40 months. In Period II (Fig. 3(b)) a maximum power also appears at the eastward component of wavenumber one with a period range of 30 to 50 months (or more broadly 20–60 months). Extremely large power is distributed in the westward moving part of wavenumber one with a period range of 100 to 200 months, but this may be due to the long-term trend, if we consider the total record length of 204 months.

Spectral distributions of wavenumber two are very similar to those of wavenumber one with smaller values in Period I and II. In Period I, considerable power is also seen at wavenumber four, but in Period II most of the power is concentrated at wavenumber one and two. The slight differences of the spectral

distribution between the two data sets may at least partly be due to the different analysis schemes used on each data set.

Fig. 4 shows the wavenumber-frequency distribution of the power spectra at 700 mb for Period II. The maximum power exists in the eastward moving component of wavenumber one with a period of 40 to 60 months. The features of the power distribution at 700 mb are very similar to those of 200 mb, though the spectra peak shifts slightly toward lower frequencies.

Krishnamurti *et al.* (1973) showed that the monthly or seasonal mean motion field in the upper troposphere consists of only major planetary-scale waves (*i.e.* wavenumbers one to three). The results here suggest that this may also be true for the inter-seasonal and interannual anomaly motion field.

The dominant time scales of these plane-

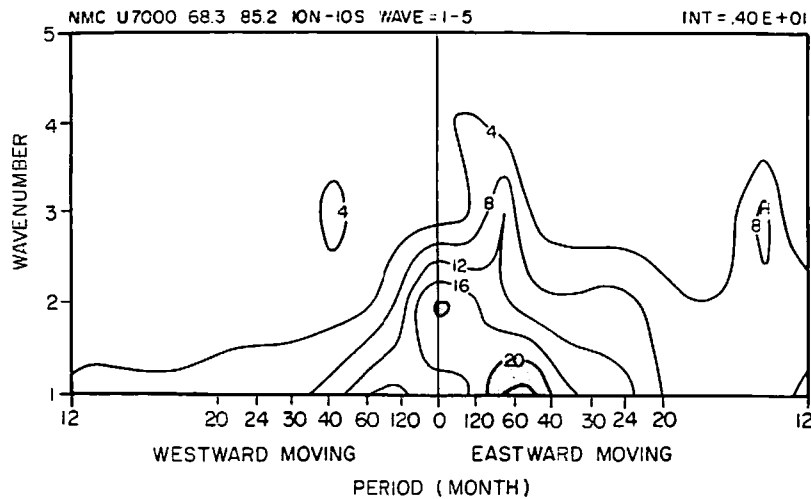


Fig. 4 Wavenumber-frequency distribution of space-time power spectra of zonal wind at 700 mb for Period II (NMC data). Units are 4 m^2 month.

tary-scale waves both at 200 mb and 700 mb are consistent with that of the SOI (Fig. 2). We may speculate, therefore, the eastward-moving planetary waves (particularly wavenumber one) may be closely associated with the SO, as noted by Pan (1979).

5. Time filter

In the following sections, we examine the longitude-time sections of the time-filtered zonal wind anomalies related to the SO. To produce the band-pass time filtered anomalies, we employed a butterworth filter (Shanks, 1967). With a proper coordinate transformation of angular frequency (ω), it is possible to construct any desired band-pass or low-pass filter without cutting both side values (Murakami, 1979).

During Period I, the SOI as well as the zonal wind at 200 mb exhibit the periodicity of about 40 months, therefore we applied the time-filter for a 30–50 month period with the maximum response at 40 months.

During period II, there appeared to be two dominant time scales in the SOI: a longer 60 month period, which may be purely associated with the frequency of El Niño events, and a shorter nearly 30 month period, which is related to the QBO. In the zonal wind anomalies, a dominant time scale appeared in a broad range of 20–60 months at both levels

(*i.e.*, 200 mb and 700 mb). However, it is important to note that this power distribution can be decomposed into the two dominant time scales (*i.e.*, a 40–60 month and 20–30 month period), if we refer to the time series as well as the power spectra of the SOI.

To deduce how the anomalies are related to the ENSO (*i.e.*, the SO with El Niño events) and to the QBO mode, two time filters for a 40–70 month period (with the maximum response at 55 month period) and for a 22–32 months period (with the maximum response at 27 months) were applied. Hereafter, we refer to the former as the SO filter and the latter as the QBO filter.

To examine the efficiency of these two filters for extracting the dominant modes, the anomalies of the SOI as well as the zonal wind deduced by the two filters are combined together to reconstruct one anomaly series. Fig. 5 shows the smoothed original SOI (solid line) and the reconstructed SOI (dashed line) for Period II. The anomalies whose time scale are shorter than a year are suppressed in the smoothed original SOI series. Although there are slight discrepancies in the magnitude between the original and reconstructed anomalies, the phase and magnitude of the overall features are quite consistent with each other.

Fig. 6 shows the time series of the smoothed original zonal wind (thick solid lines) and

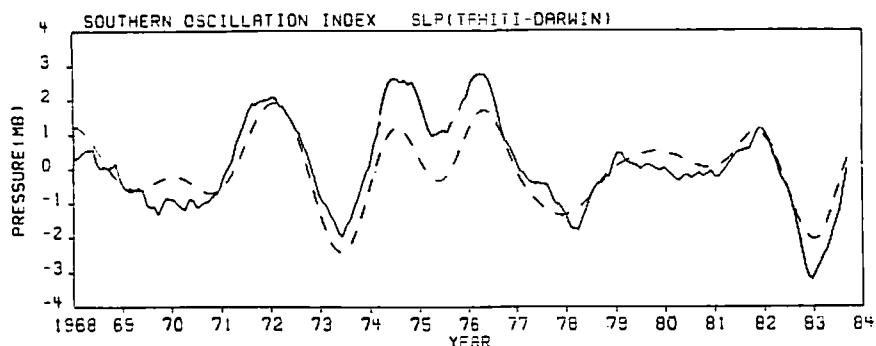


Fig. 5 11-month moving averaged SOI (solid line) and reconstructed SOI (dashed line) by composing two time-filtered anomalies for Period II (NMC data).

the reconstructed zonal wind (solid lines) at 200 mb for the six longitude blocks along the equator. The anomalies deduced purely by the SO filter are also indicated with dashed lines.

There is little doubt that the reconstructed zonal winds represent the smoothed original zonal wind fluctuations, particularly over the whole Pacific Ocean area. Even over the Indian Ocean (30°E–60°E), where considerable discrepancy in the magnitude exists between the two time series, the anomalies with the time scale of the SO and/or QBO are still apparent in the both series.

Thus, these two time filters for Period II seem to be suitable to deduce the dominant modes of interannual time scale in the anomaly wind field.

6. Longitude-time structure related to the SO

a. Zonal wind field

In this section, we discuss the anomaly field deduced by the SO filter. Fig. 7 shows the longitude-time section of the filtered zonal wind at 200 mb along the equatorial belt (10°S to 10°N) for Period I, and Fig. 8 shows those of (a) 200 mb and (b) 700 mb for Period II. The maximum phases of the SOI in the filtered time series (Fig. 5) are also shown. Through Period I and II, the eastward propagation of the anomalies with approximately wavenumber-one structure is clearly shown. The eastward propagation is more evident from the Indian Ocean through the eastern Pacific (90°E to 60°W), whereas nearly simul-

taneous change of the anomalies are dominant over the other regions (*i. e.*, South America, Africa and the Atlantic Ocean).

Another remarkable feature especially in Period II (Fig. 8) is the amplification of the anomalies over the central through the eastern Pacific (110°E to 100°W). The maximum (minimum) anomalies appear to be consistent with the maximum (minimum) phases of the SOI. In Period I (Fig. 7), the maximum (minimum) anomalies shift more westward or, in other words, the anomalies are weaker over the eastern Pacific (180°W to 100°W). This is most likely due to zero-anomaly bogus points over this data-sparse region, which were added to the original data in order to suppress artificially-produced extremely large anomalies during the interpolation. A standing-type oscillation is, instead, more pronounced over the region from Indonesia through the central Pacific in Period I, while in Period II the anomalies over the eastern hemisphere are generally small. These differences in the anomaly patterns of the two data sets may be attributed to the use of different analysis schemes. However, the overall anomaly patterns of the two data sets seem to be quite similar to each other for the overlapped period.

At the maximum (minimum) SOI phase, the westerly (easterly) anomalies are dominant over a broad area to the west of Indonesia (about two thirds of the entire global belt), while the easterly (westerly) anomalies are limited to the central and the eastern Pacific. This zonal asymmetry in the 200 mb zonal wind anomalies at the maximum (minimum)

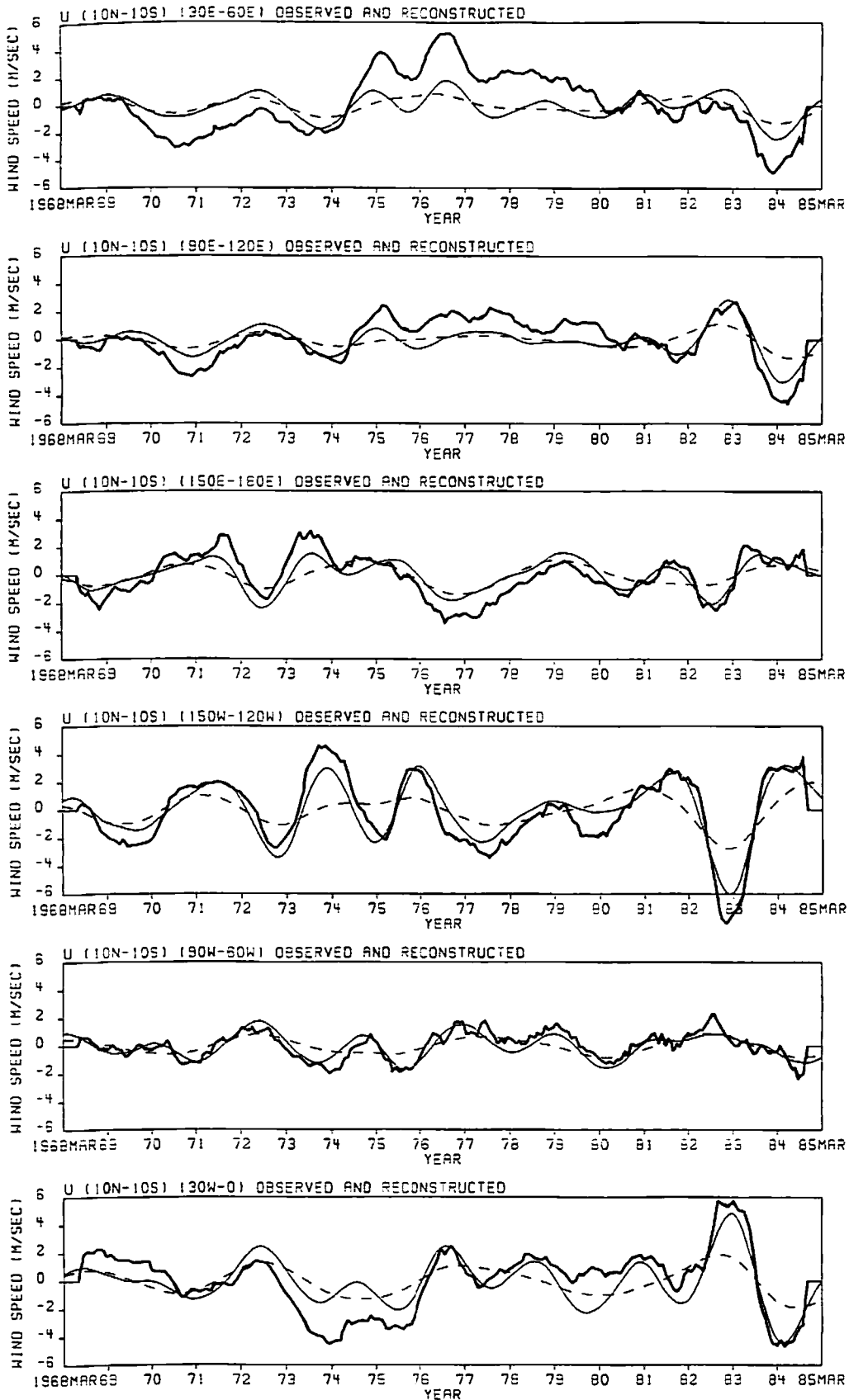


Fig. 6 11-month moving averaged zonal wind (thick solid line), reconstructed zonal wind from the two time-filtered anomalies (solid line) and zonal wind anomaly from the SO filter (dashed line) at 200 mb for the six longitude blocks (30°E-60°E, 90°E-120°E, 150°E-180, 150°W-120°W, 90°W-60°W, 30°W-0) along the equatorial belt (10°N-10°S).

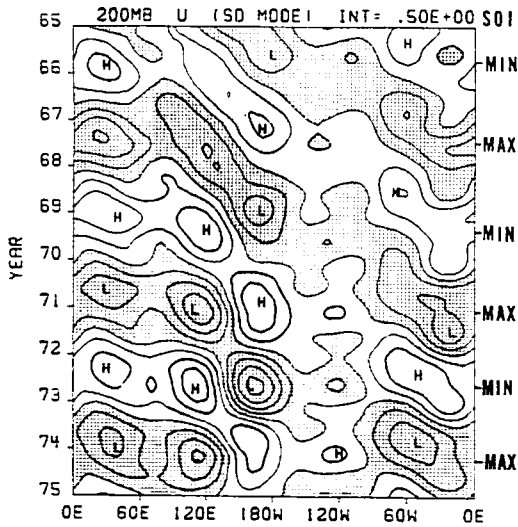


Fig. 7 Longitude-time section of filtered zonal wind of the SO mode at 200 mb ($10^{\circ}\text{N}-10^{\circ}\text{S}$) for Period I (FSU data). Units are 0.5 m sec^{-1} . Maximum and minimum phases of the filtered SOI are also shown with "MAX" and "MIN". Negative (easterly) anomalies are shaded.

SO phases are essentially identical with the previous results of Arkin (1982) and Selkirk (1984).

The zonal wind anomalies at 700 mb for Period II (Fig. 8(b)) shows a very similar pattern to those of 200 mb (Fig. 8(a)) but with the opposite sign, though there is some minor noise present. That is, the westerly (easterly) anomalies are well coupled to the easterly (westerly) anomalies at 200 mb. The combination of the anomalies at 200 mb and 700 mb presents an evidence of eastward-propagating east-west circulation with wavenumber one (or two-cell) structure in the anomaly tropical motion field associated with the ENSO phenomenon.

The westerly (easterly) maximum, *i. e.* the weakest (strongest) easterly jet, over the Indian Ocean appears nearly simultaneously with, or by one or two seasons ahead of the

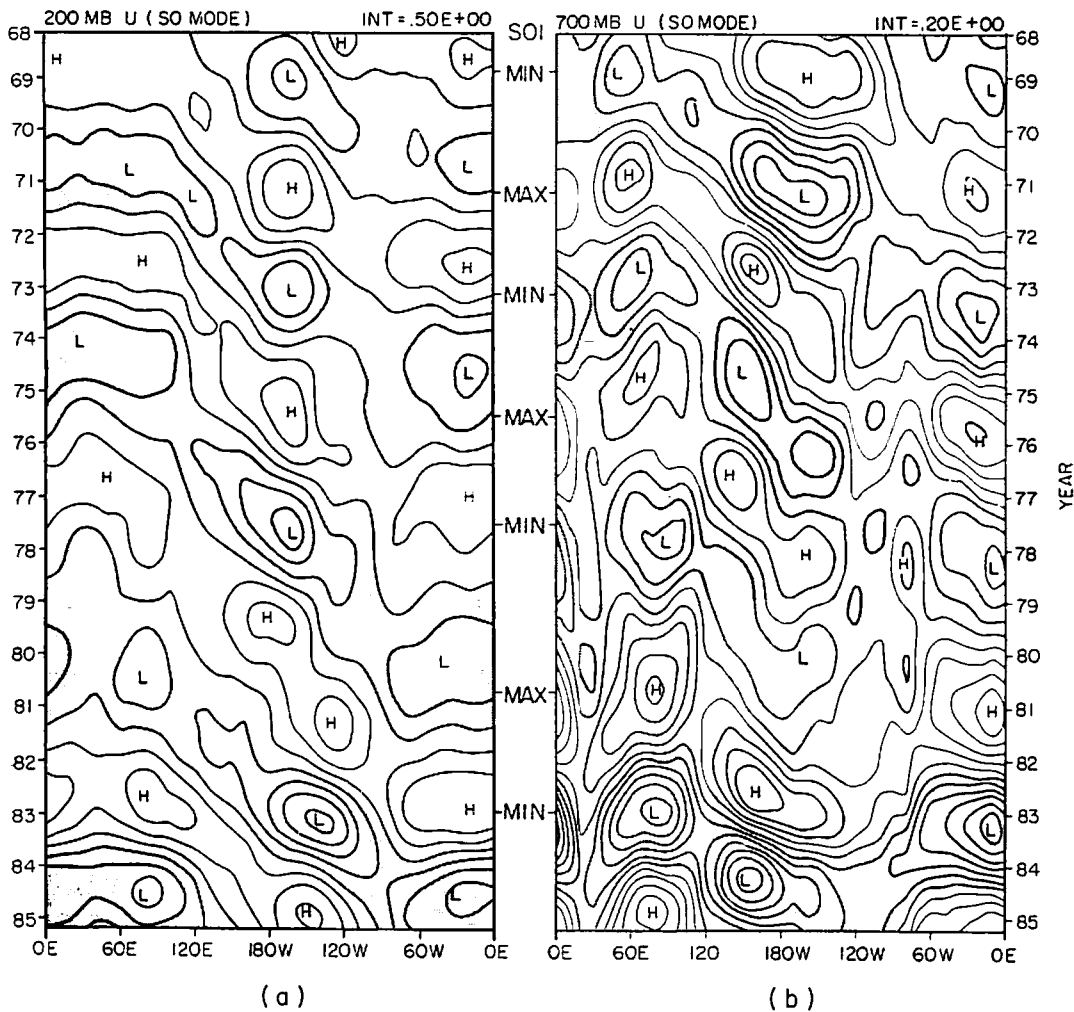


Fig. 8 Same as Fig. 7 but for Period II. Units are (a) 0.5 m sec^{-1} and (b) 0.2 m sec^{-1} . Negative (easterly) anomalies are shaded.

easterly (westerly) maximum over the central through eastern Pacific. The easterly (westerly) maximum over the Pacific region corresponds to the strongest (weakest) convection over there (Arkin, 1982). These anomaly patterns may imply, therefore, that the weak (strong) monsoon over India is coupled nearly in phase to, or slightly prior to the strong (weak) convection over the central through eastern Pacific.

Some studies (Pant and Parthasarathy, 1981; Rasmusson and Carpenter, 1983; Bhalme and Jadhav, 1984) showed the high positive correlation between the monsoon rainfall over India and the SOI. Bhalme and Jadhav (1984) suggested that there are also significant lag-correlations of one to three seasons where the monsoon rainfall precedes the SOI. It is true that during the period of the present analysis (1965-85), all of the El Niño events (near the minimum SOI) were preceded without exception by the weaker than normal Indian summer monsoons (of 1965, 1969, 1972, 1976 and 1982). This observational evidence appears to be consistent with the zonal wind anomalies described here.

The zonal wind anomalies over South America through the western Indian Ocean (60°W-60°E), which may be associated mainly with the convective activities over equatorial South America (the Amazon Basin and northeast Brazil) and Africa (the Congo Basin), show nearly in-phase variations. The easterly (westerly) anomalies at 200 mb may correspond with above (below) normal convection over these regions. Since the zonal wind anomalies over these region are negatively correlated with that over the eastern Pacific, the convection over these two regions may be negatively correlated with that over the eastern Pacific. Stockenius (1981) deduced the same correlations by using precipitation data over these regions. Some recent studies (Lau and Chan, 1983; Ardanuy, 1985) have also shown a significant negative correlation between the equatorial central Pacific and the equatorial south America in the outgoing longwave radiation (OLR) anomalies associated with the ENSO events.

Thus, the fluctuations of Indian summer

monsoon and convective activities over the Pacific, south America and Africa in the equatorial zone seem to be positively or negatively highly correlated with each other. This may form, as a whole, a "transient-type" structure of the global east-west circulation in the anomaly zonal wind field.

During 1980 to 1983, the large anomalies over the central Pacific seem to be located about 30° of longitude to the east of the normal (or previous years) position. This may be associated with the abnormally intensified and eastward extended area of convection during the El Niño 1982/83 (Lau and Chan, 1985 *etc.*)

It may be worthwhile to note that the eastward-propagation as well as the zonal asymmetry on the anomaly zonal wind described here will give us a somewhat different picture of the heat-induced tropical circulation from the simplified models (Gill, 1980; Geisler, 1981). We will discuss this problem further in section 9.

b. velocity potential

The velocity potential (or divergent wind) field has proven to be a more useful measure to identify planetary-scale divergent circulations than the original wind field. The intensities of east-west circulation and meridional (or Hadley) circulation are estimated from the zonal and meridional gradients of the velocity potential field, respectively. In the anomaly (from the normal) velocity potential field, the interseasonal as well as interannual variations of the divergent circulations are described by Krishnamurti *et al.* (1985).

There may be a few problems in obtaining the velocity potential field. One problem may be its dependency on the computational method used to generate velocity potential. Since the spatial data coverage used in this study is limited in the lower latitudes, the boundary conditions may also have some impact on the results. For example, the boundary condition $\chi=0$ (χ : velocity potential) set in the northern and southern lower latitudes may apparently stress the meridional circulation. Another problem may be its large dependency on the analysis scheme with which the original wind

field was produced. For example, some part of the NMC data was produced by using Hough analysis, which contains fundamentally no divergent part of the wind (Arkin, 1982).

In this study, to minimize the boundary effects as well as computation time, the double Fourier transform method (Stephens and Johnson, 1978) was used to compute the velocity potential. This method assumes cyclic boundary conditions for a rectangular domain. The cyclic boundary conditions may result in some deformation of the field near the northern and the southern boundaries. However, as the main area of interest in this study is the tropical belt (15°N-15°S), this should not cause serious errors in the results. Since the data sets used here were derived from different data source with four different analysis schemes, the results described here may still be tentative.

Fig. 9 shows the longitude-time section of the filtered velocity potential at 200 mb along the tropical belt (15°N-15°S) for Period I. The velocity potential here is defined as

$$\nabla^2\chi = -\nabla \cdot V$$

(χ : velocity potential, V : wind vector) so that the maximum value shows a center of divergent wind.

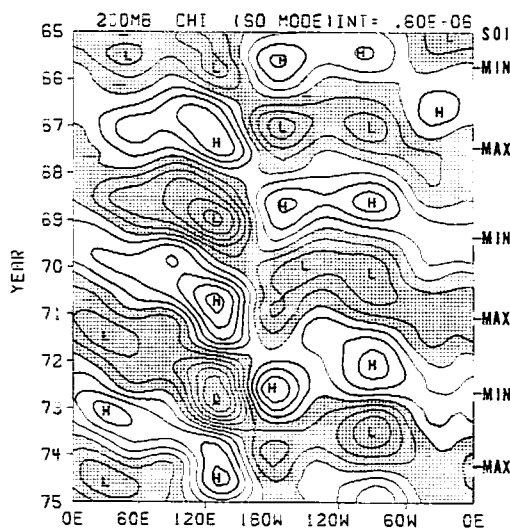


Fig. 9 Longitude-time section of the filtered velocity potential of the SO mode at 200 mb (15°N-15°S) for Period I (FSU data). Units are $6 \times 10^5 \text{ m}^2 \text{ sec}^{-1}$. Negative anomalies are shaded. Maximum and minimum phases of the filtered SOI are also shown with "MAX" and "MIN".

An eastward-propagating wavenumber-one structure is again a salient feature, and is consistent with the zonal wind field (Fig. 7). Another interesting feature is a strong amplification of the anomalies with the opposite sign between the Asian monsoon region and the central/eastern Pacific or, in other words, a standing-type oscillation between these two regions.

In addition to the zonal wind anomalies, the maximum (minimum) velocity potential over the monsoon region (120°E-150°E) correspond well with the maximum (minimum) phases of the SOI. This standing-type oscillation apparently represents weakening or strengthening of the local Walker circulation over the Pacific (Bjerknes, 1969), although the anomalies over the eastern Pacific are underestimated as mentioned in the previous section.

Fig. 10 shows the longitude-time section of the filtered velocity potential at (a) 200 mb and (b) 700 mb for Period II. The data for September 1974 through August 1978 was omitted, since the data was produced by Hough analysis which is fundamentally non-divergent. During the period from March 1968 through August 1974 at 200 mb, any zonal propagation failed to appear, although the result at 700 mb for the same period in Fig. 9 shows evidence of an apparent eastward propagation. The anomalies of the divergent zonal wind ($= -\partial\chi/\partial x$) show, however, a systematic eastward propagation from the Indian Ocean through the eastern Pacific (not shown here). During the period from September 1978 through February 1985, the eastward propagation is evident with large amplitudes over the region from the Indian Ocean through the eastern Pacific (60°E-120°W). The maximum (minimum) and the minimum (maximum) anomalies are located over the Indonesian maritime continent and the eastern Pacific respectively, in phase with the maximum (minimum) phases of the SOI.

The same diagram for 700 mb (Fig. 10(b)) clearly shows an eastward propagation of the anomalies with wavenumber-one structure through the entire analysis period. The anomaly pattern is very similar to that at 200 mb with the opposite sign especially after 1978,

7. Longitude-time structure related to the QBO

As described above, the QBO mode is another dominant mode in the SOI particularly during Period II. The time-space spectral analysis has also suggested that a considerable amount of power exists in the period range of the QBO. To examine the zonal structure of the QBO mode and its association with the SO, the QBO filter described in section 5 is applied to the zonal wind anomalies.

Fig. 11 shows the longitude-time section of the zonal wind anomalies of the QBO mode at (a) 200 mb and (b) 700 mb along the equatorial belt (10°N - 10°S). A remarkable feature at both levels is the eastward propagation of

the wavenumber-one structure, which is very similar to the SO mode except for the phase speed. The phase speed of this mode is 12° - 15° long. month $^{-1}$, whereas that of the SO is 6° - 10° long. month $^{-1}$. At 200 mb, maximum amplitudes seem to be fixed over the Pacific region (120°E - 90°W), but secondary maximum also appear over the Atlantic Ocean, west Africa and over the Indian Ocean through Indonesia. At 700 mb, the standing-oscillation component is also apparent between the Indian Ocean/Indonesian region and the central Pacific.

This mode seems to exhibit a large inter-annual trend in the amplitude fluctuation. During the period from 1971 through 1977 and from 1980 through 1985, large amplifications with systematic zonal propagation are

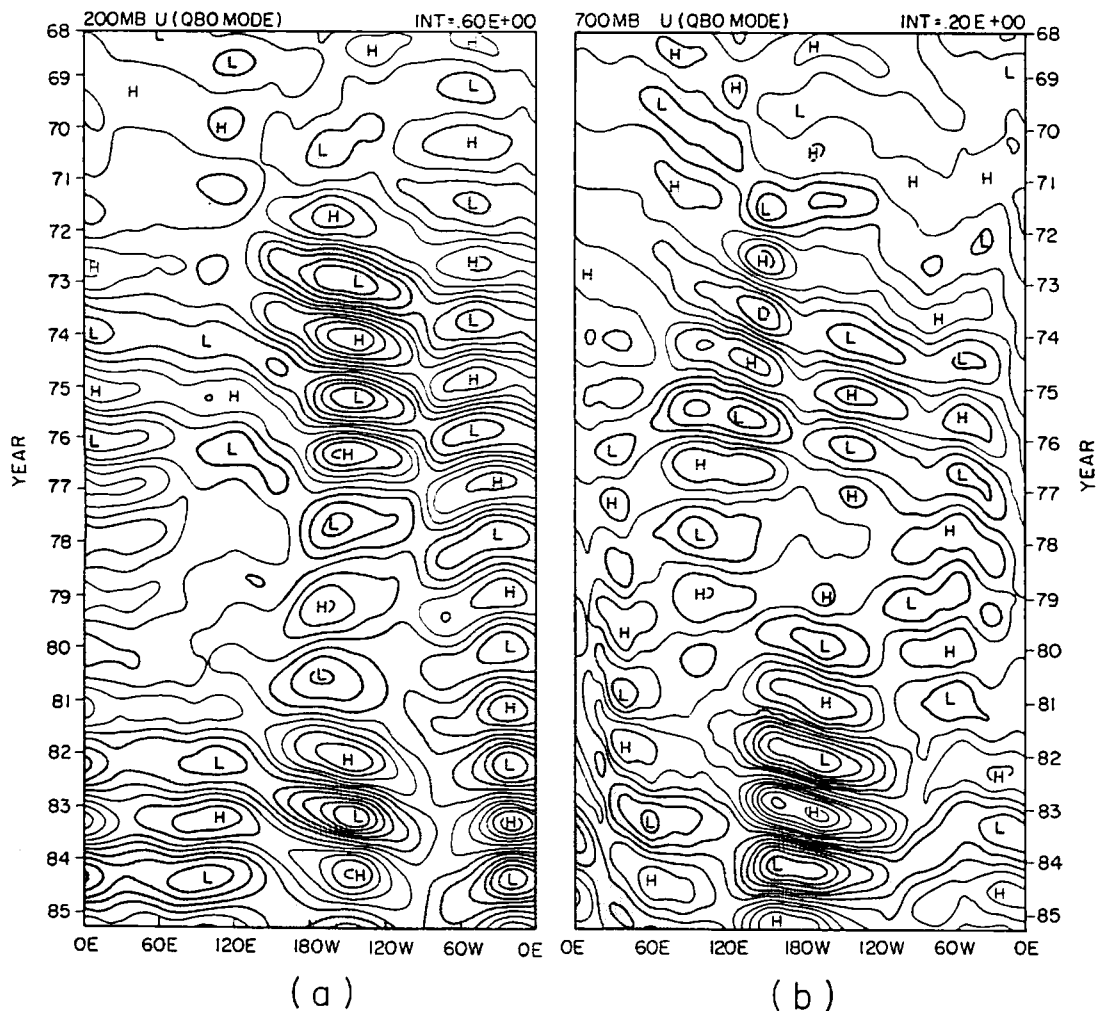


Fig. 11 Longitude-time section of the filtered zonal wind of the QBO mode (10°N - 10°S) for Period II (NMC data) at (a) 200 mb and (b) 700 mb. Units are (a) 0.6 m sec^{-1} and (b) 0.2 m sec^{-1} . Negative (easterly) anomalies are shaded.

noticeable at both levels, while during the other period the signals of this mode are weak.

As well as the SO mode, the anomalies of the two levels (200 mb and 700 mb) in time-space field suggest that this mode has the structure of the anomalous east-west circulation cell, since the easterly (westerly) anomalies at 200 mb are nearly consistent with the westerly (easterly) anomalies at 700 mb.

8. Coupling between the SO and the QBO

The combined effect of the SO and the QBO mode may represent more realistic anomalies associated with the SO particularly during Period II, since the amplitudes of the QBO seem to be comparable with or even larger than those of the SO mode. This has been evidenced for the SOI and the zonal wind as shown in Fig. 5 and Fig. 6.

Fig. 12 shows the longitude-time section of the maximum easterly wind anomalies at 200 mb for the SO mode (solid line) and the QBO mode (dashed line), reproduced from Fig. 8(a) and Fig. 11(a). Interestingly, whether El Niño events (near the minimum SOI phase) become major ones (*e.g.*, 1972/73 and 1982/83) or otherwise minor ones (*e.g.*, 1969 and 1976/77), seem to depend upon the coupling or decoupling of the large easterly anomalies in the SO and the QBO mode. The absence of El Niño event in 1975, although the SOI itself is diminished considerably (see Fig. 1), may also be explained by the offset coupling of the maximum westerly anomalies in the SO mode and the maximum easterly anomalies in the QBO mode. Furthermore, a pronounced anti-El Niño condition (*i.e.* very strong convection over the Indonesian region), which has been observed in the OLR anomalies (Bergman and Quiroz, 1984), is also shown to be composed of the easterly anomalies of the two modes between 80°E–120°E. Thus, the occurrence or absence of a major or minor El Niño event seems to be well correlated to the interaction of these two modes.

The problem still remains as to whether the SO and the QBO mode in the planetary-scale east-west circulations in the tropics are

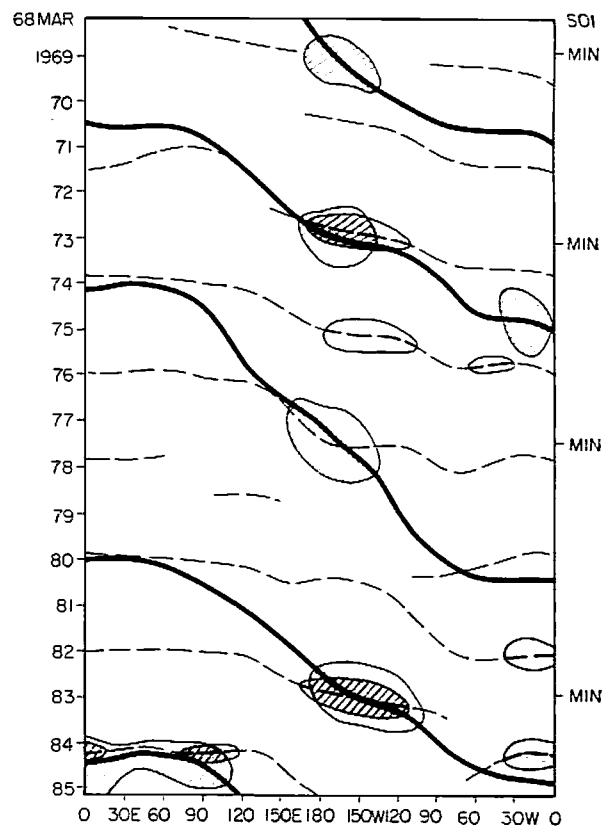


Fig. 12 Composite longitude-time section of the filtered maximum easterlies at 200 mb for the SO mode (solid line) and the QBO mode (dashed line). Anomalies of more than 1.5 m sec^{-1} for each mode are displayed with hatched and stippled area. Minimum phases (El Niño phases) of the filtered SOI are also shown with "MIN".

derived from different forcing mechanisms. At least phenomenologically, however, it may be more reasonable to treat these two modes as independent of each other, since each mode in the zonal wind field shows systematic time-space anomalies with different phase speeds.

A number of previous studies have already presented evidences of strong coherency and persistency of the QBO mode in tropospheric wind, pressure, temperature, rainfall, SST and other parameters in most of the tropical regions (*e.g.*, Tyson *et al.*, 1975; Hastenrath and Kaczmarczyk, 1981; Yasunari, 1981; Barnett, 1983; Bhalme and Jhadav, 1984; Nicholson and Entekhabi, 1985 *etc.*). It may be probable, therefore, that the QBO is one of the predominant normal mode fluctuations in the tropical troposphere (as well as in the

stratosphere) and that it sometimes functions as a carrier wave of the anomalies on longer-time scales.

9. Summary and discussion

The global-scale east-west circulation in the tropics associated with the SO has been investigated by using zonal wind and velocity potential fields in the upper and the lower troposphere constructed from the two different wind data sets.

Although there is a strong seasonal dependence of the SO signals in the various meteorological fields as noted in many previous studies (*e.g.*, Horel and Wallace, 1981; Rasmusson and Carpenter, 1982 *etc.*), the strong persistence of the anomalies from season to season or throughout the year should also be emphasized, particularly focusing on the time evolution of the entire SO cycle. The time-filtering method adopted here has proven to be successful, in this sense, since it not only extracts the interseasonal and interannual persistent anomalies but it also fundamentally preserves their seasonalities. (For example, the maximum or minimum zonal wind anomalies over the Pacific in Fig. 7 and Fig. 8 appear mostly during the colder seasons in the northern hemisphere as noted in the previous observations.)

An eastward-propagating anomalous divergent circulation was found on the time scale of the SO (40–60 month period) with a zonal wavenumber-one structure. This mode shows an amplification and/or a standing-type oscillation of the anomalies over the region from Indonesia through the eastern Pacific, which may correspond with the modulation of the local Walker circulation originally noted by Bjerknes (1969). Another east-west circulation with a similar zonal structure and phase-propagation has also been detected on the QBO time scale. In addition, these two modes are suggested to be coupled (decoupled) associated with the major (minor) El Niño events over the eastern Pacific.

Very recently, Barnett (1983; 1984a; 1984b; 1985) and Krishnamurti *et al.* (1985) showed that the surface wind and pressure anomalies move eastward from the Indian Ocean to the

Pacific region associated with the SO. Arkin *et al.* (1983) also showed the eastward movement of the anomalies in the sea surface temperature, 850 mb and 200 mb zonal wind, and the OLR, although their analysis is limited to two years during the 1982/83 ENSO period.

Their findings may be closely related to the eastward-propagating mode in the upper and lower troposphere discussed here. For example, the surface zonal wind anomalies (see Fig. 8 of Barnett, 1983) is propagating nearly in phase which that at 700 mb (Fig. 8(b)). The positive (negative) pressure anomalies (see Fig. 12 in Krishnamurti *et al.*, 1984) also show nearly in-phase propagation with the easterly (westerly) anomalies at 700 mb. These observational evidences further support the existence of the eastward-propagating east-west circulation along the equator. Furthermore, the remarkable circulation anomalies in the upper and the lower troposphere over the Indian Ocean described above lead us to speculate the SO over the Pacific may be closely linked with the monsoon circulation over the Indian Ocean region. Very recently, Cadet (1985) showed a strong association between the SOI and the surface field over the Indian Ocean. Barnett (1984b) also proposed this link of the SO with the summer monsoon over India from the analysis of the surface pressure and wind field.

Some theoretical studies on heat-induced tropical circulations (*e.g.*, Gill, 1980; Geisler, 1981) show a zonal asymmetry of the stationary zonal wind field, which seem to have simulated successfully the real wind field over Indonesia through the Pacific region. Some studies (McWilliams and Gent, 1978; McCreary, 1983; Hastenrath and Wu, 1982; Wright, 1979 *etc.*) have also tried to construct a dynamical model of the SO as an atmosphere-ocean coupled system over the equatorial Pacific. However, these models failed to simulate the eastward propagation of the anomalies from the Indian Ocean toward the eastern Pacific, which is an important observational aspect deduced here.

Philander *et al.* (1984) recently proposed an atmosphere-ocean coupled model which shows an eastward propagation of the surface zonal

wind as well as the SST anomalies from the western Pacific to the eastern Pacific. The observed phase speed of the zonal wind anomalies (Fig. 8) are well consistent with that in their model. The eastward propagation of the east-west circulation described here may be at least in part explained by their dynamics: *i. e.*, the dominant role of the oceanic Kelvin waves to the west of the maximum convection. However, their model does not explain how the initial perturbation occurs over the western Pacific (or the Indonesian region). In this context, the zonal wind anomalies over the Indian Ocean as observed in this study may be important.

A possible link between the Indian Ocean and the Pacific may be postulated as follows: a weakening of Indian summer monsoon (*i. e.*, weakening of the easterly jet over the Indian Ocean) by some mechanism leads to a weakening of the east-west circulation over the Indian Ocean through the Indonesian maritime continent, which results in a weakening of the convective activity over the maritime continent with some phase lag. The weakening of the convection over the maritime continent leads to a weakening of the trade wind system again with some phase lag *via* the Walker circulation, which finally trigger the SST warming over the central through the eastern Pacific. This leads to the ENSO event as a number of the studies have already described. At this stage, the anomalous east-west (or Walker) circulation is completely reversed. However, many fundamental questions still remain unanswered such as how the new anomalies (with the opposite sign) appear over the Indian Ocean, and how the anomalies can persist for a year or more even over the monsoon region where a strong seasonality exists.

In summary, the present study offered an evidence that the SO is a part of the combined circulation systems over the whole tropics. Particularly, the eastward propagation of the zonal as well as divergent wind anomalies from the Indian Ocean toward the eastern Pacific prompts us to investigate further about the link between the monsoon circulation over Asia and the Walker circulation over the

Pacific as a land-atmosphere-ocean coupled system. This system, in addition, should form an integral part of a global climate system which has a preferred time scale of several years. To approach this problem, global data sets of the circulation anomalies as well as the SST anomalies, which cover about twenty years (of several SO cycles) are being processed.

Another interesting aspect of the zonally-propagating mode described here may be a similarity of its spatial structure of the propagation to the 30-50 day mode divergent circulation over the global tropics (Madden and Julian, 1972; Lorenc, 1984; Krishnamurti *et al.*, 1984 *etc.*). The association between these two low-frequency modes also deserves to be studied.

Acknowledgements

The author would particularly like to thank Prof. T.N. Krishnamurti for his great support, encouragement and stimulating discussions throughout the work. He is also indebted to Dr. Eugene M. Rasmusson and Dr. P.A. Arkin for providing the NMC tropical wind data set. Thanks are due to Mr. J. Manobianco in editing the manuscript. The research reported here is supported by NOAA Grant No. NA85AA-H-CA019.

References

- Ardanuy, P.E., 1985: The 1982/83 El Niño and outgoing longwave radiation. *Proc. 16th Conf. Hurricane and Tropical Met.*, May 1985, Houston, Texas.
- Arkin, P.A., 1982: The relationship between inter-annual variability in the 200 mb tropical wind field and the Southern Oscillation. *Mon. Wea. Rev.*, 110, 1393-1404.
- , J.D. Kopman and R.W. Reynolds, 1983: *1982-1983 El Niño/Southern Oscillation Event Quick Look Atlas*. Climate Analysis Center, NMC, NWS, NOAA.
- Barnett, T.P., 1983: Interaction of the monsoon system and Pacific trade wind system at inter-annual time scales. Part I: The equatorial zone. *Mon. Wea. Rev.*, 111, 756-773.
- , 1984a: Interaction of the monsoon system and Pacific trade wind system at inter-annual time scales. Part II: The tropical band. *Mon. Wea. Rev.*, 112, 2380-2387.
- , 1984b: Interaction of the monsoon sys-

- tem and Pacific trade wind system at inter-annual time scales. Part III: A Partial anatomy of the Southern Oscillation. *Mon. Wea. Rev.*, 112, 2388-2400.
- , 1985: Variations in near-global sea level pressure. *J. Atmos. Sci.*, 42, 478-501.
- Bergman, K. and R. Quiroz, 1984: Review of the climate of fall 1983 and winter 1983-84. *Proc. 9th Ann. Conf. Climate Diagnos. Workshop*, Corvallis, Oregon, 21-31.
- Bhalme, H. N. and S. K. Jadhav, 1984: The Southern Oscillation and its relation to the monsoon rainfall. *J. Climat.*, 4, 509-520.
- Bjerknes, J., 1969: Atmospheric teleconnections from the equatorial Pacific. *Mon. Rev. Rev.*, 97, 163-172.
- Brier, G. W., 1978: The quasi-biennial oscillation and feedback processes in the atmosphere-ocean earth system. *Mon. Wea. Rev.*, 106, 938-954.
- Cadet, D. L., 1985: The Southern Oscillation over the Indian Ocean. *J. Climat.*, 5, 189-212.
- Geisler, J. E., 1981: A linear model of the Walker circulation. *J. Atmos. Sci.*, 38, 1390-1400.
- Gill, A. E., 1980: Some simple solutions for heat-induced tropical circulation. *Quart. J. Roy. Meteor. Soc.*, 106, 447-462.
- Hastenrath, S. and E. B. Kaczmarczyk, 1981: On spectra and coherence of tropical climate anomalies. *Tellus*, 33, 453-462.
- and M.-C. Wu, 1982: Oscillations of upper-air circulation and anomalies in the surface climate of the tropics. *Archiv. Met. Geoph. Biokl.*, Ser. B, 31, 1-37.
- Hayashi, Y., 1977: Space-time power spectral analysis using the maximum entropy method. *J. Meteor. Soc. Japan*, 55, 415-420.
- Horel, J. D. and J. M. Wallace, 1981: Planetary-scale atmospheric phenomena associated with the Southern Oscillation. *Mon. Wea. Rev.*, 109, 813-829.
- Kanamitsu, M. and T. N. Krishnamurti, 1978: Northern summer tropical circulations during drought and normal rainfall years. *Mon. Wea. Rev.*, 106, 31-47.
- Krishnamurti, T. N., 1971: Tropical east-west circulations during the northern summer. *J. Atmos. Sci.*, 28, 1342-1347.
- , M. Kanamitsu, W. S. Koss and J. D. Lee, 1973: Tropical east-west circulations during the northern winter. *J. Atmos. Sci.*, 30, 780-787.
- , Hua-L. Pan, R. Pasch and D. Subrahmanyam, 1983: Interannual Variability of the tropical motion field. Florida State University Report No. 83-3.
- , N. Surgi and J. Manobianco, 1985: Recent results on divergent circulations over the global tropics. (To be published in *J. Meteor. Res.*)
- , P. K. Jayakumar, J. Sheng, N. Surgi and A. Kumar, 1985: Divergent circulations on the 30 to 50 day time scale. (To be published in *J. Atmos. Sci.*, 42, No. 2.)
- , Shao-H. Chu and W. Iglesias, 1985: On the sea level pressure of the Southern Oscillation. (To be published in *Arch. Met. Geoph. Biokl.*, Ser. A.)
- Lau, K. M. and Chan, P. H., 1983: Short-term climate variability and atmospheric teleconnections from satellite-observed outgoing longwave radiation. Part I: Simultaneous relationships. *J. Atmos. Sci.*, 40, 2735-2750.
- and ———, 1985: Aspects of the 40-50 day oscillation as inferred from outgoing longwave radiation. *Mon. Wea. Rev.* (in press).
- Lorenc, A. C., 1984: The evolution of planetary-scale 200 mb divergent flow during the FGGE year. *Quart. J. Roy. Met. Soc.*, 110, 427-441.
- Madden, R. A. and P. R. Julian, 1972: Description of global scale circulation cells in the tropics with a 40-50 day period. *J. Atmos. Sci.*, 29, 1109-1123.
- McCreary, J. P., 1983: A model of tropical ocean-atmosphere interaction. *Mon. Wea. Rev.*, 111, 370-387.
- McWilliams, J. C. and P. R. Gent, 1978: A coupled air-sea model for the tropical Pacific. *J. Atmos. Sci.*, 35, 962-989.
- Murakami, M., 1979: Large scale aspects of deep convective activity over the GATE area. *Mon. Wea. Rev.*, 107, 994-1013.
- Nicholls, N., 1978: Air-sea interaction and the quasi-biennial oscillation. *Mon. Wea. Rev.*, 106, 105-108.
- Nicholson, S. and D. Entekhabi, 1985: The quasi-periodic behaviour of rainfall variability in Africa and its relationship to the Southern Oscillation. (To be published in *Arch. Met. Geoph. Biokl.*, Ser. A.)
- Pan, Hua-L., 1979: *Upper tropospheric tropical circulations during a recent decade*. Ph. D. Thesis at Florida State University. 142pp. (also available from FSU report No. 79-1.)
- Pant, G. B. and B. Parthasarathy, 1981: Some aspects of an association between the Southern Oscillation and Indian summer monsoon. *Arch. Met. Geoph. Biokl.*, Ser. B, 29, 245-252.
- Philander, S. G. H., T. Yamagata and R. C. Pacanowski, 1984: Unstable air-sea interactions in the tropics. *J. Atmos. Sci.*, 41, 604-613.
- Rasmusson, E. M. and T. H. Carpenter, 1982: Variations in tropical sea surface temperature and surface wind fields associated with the Southern Oscillation/El Niño. *Mon. Wea. Rev.*, 110, 354-384.
- and ———, 1983: The relation between eastern equatorial Pacific sea surface temperature and rainfall over India and Sri Lanka. *Mon. Wea. Rev.*, 111, 517-528.
- Selkirk, R., 1984: Seasonally stratified correlations of the 200 mb tropical wind field to the Southern

- Oscillation. *J. Climat.*, 4, 365-382.
- Shanks, J.L., 1967: Recursion filters for digital processing. *Geophysica*, 32, 33-51.
- Stephens, J.J. and K.W. Johnson, 1978: Rotational and divergent wind potentials. *Mon. Wea. Rev.*, 106, 1452-1457.
- Stockenius, T., 1981: Interannual variations of tropical precipitation patterns. *Mon. Wea. Rev.*, 109, 1233-1247.
- Trenberth, K.E., 1975: A quasi-biennial standing waves in the southern hemisphere and interactions with sea surface temperature. *Quart. J. Roy. Met. Soc.*, 101, 55-74.
- , 1976: Spatial and temporal variations of the Southern Oscillation. *Quart. J. Roy. Soc.*, 102, 636-653.
- Tyson, P.D., T.G.J. Dyer and M.N. Mametse, 1975: Secular changes in South African rainfall: 1880 to 1972. *Quart. J. Roy. Met. Soc.*, 101, 817-832.
- Wright, P.B., 1973: A simple model for simulating regional short-term climatic changes. *Mon. Wea. Rev.*, 107, 1567-1580.
- Yasunari, T., 1981: Temporal and spatial variations of monthly rainfall in Java, Indonesia. *Southeast Asian Studies (Tonan Ajia Kenkyu)*, 19, 170-186.

Southern Oscillation (南方振動) に伴う熱帯東西循環の伝播モード

安成哲三*

フロリダ州立大学気象学教室

Southern Oscillation (SO) に関連した熱帯東西循環の変動を、20年間 (1965-84) の熱帯全域風資料 (FSU 及び NMC 作製) を用いて調べた。

対流圏上層・下層の東西風成分には、SO の周期 (40-60ヶ月) に対応して、東進する波数1の波が卓越していることが明らかとなった。この波は、上層 (200 mb) と下層 (700 mb) で逆位相を示し、熱帯全域で2つのセル構造を持つ東西循環の東進成分として捉えることができる。速度ポテンシャル場の解析からも、この様相は示された。東進の位相 (位相速度: 6° - 10° 経度/月) と振幅は、インド洋から東部太平洋にいたる地域で最も顕著に現われる。

東西循環の変動の、もうひとつの卓越モードとして、準2年周期振動 (QBO) も確認された。東西方向の構造は、SO モードと同様の東進する波数1の波の構造を示すが、位相速度 (12° - 15° 経度/月) は SO モードより速い。

さらに、中・東部太平洋におけるエル・ニーニョ現象の発現・不発現又はその強弱は、東西風成分に現われた上記ふたつのモード (SO モードと QBO モード) の相互作用により調節されている可能性が示唆された。

* 現在所属: 筑波大学地球科学系